

## Observation of local non-centrosymmetry in weakly biferroic $\text{YCrO}_3$

This article has been downloaded from IOPscience. Please scroll down to see the full text article.

2007 J. Phys.: Condens. Matter 19 102202

(<http://iopscience.iop.org/0953-8984/19/10/102202>)

View [the table of contents for this issue](#), or go to the [journal homepage](#) for more

Download details:

IP Address: 129.252.86.83

The article was downloaded on 28/05/2010 at 16:29

Please note that [terms and conditions apply](#).

## FAST TRACK COMMUNICATION

# Observation of local non-centrosymmetry in weakly biferroic $\text{YCrO}_3$

K Ramesha<sup>1</sup>, A Llobet<sup>1</sup>, Th Proffen<sup>1</sup>, C R Serrao<sup>2</sup> and C N R Rao<sup>2</sup><sup>1</sup> Lujan Neutron Scattering Center, Los Alamos National Laboratory, Los Alamos, NM 87545, USA<sup>2</sup> Chemistry and Physics of Materials Unit, Jawaharlal Nehru Centre for Advanced Scientific Research, Jakkur PO, Bangalore 560 064, India

Received 27 November 2006, in final form 31 January 2007

Published 23 February 2007

Online at [stacks.iop.org/JPhysCM/19/102202](http://stacks.iop.org/JPhysCM/19/102202)**Abstract**

Using high-resolution neutron powder diffraction we have determined the average and local structure of  $\text{YCrO}_3$  in order to explain the recently reported properties of  $\text{YCrO}_3$ .

Unlike conventional ferroelectric systems,  $\text{YCrO}_3$  is reported to possess a centrosymmetric crystal structure which is inconsistent with the development of weak electric polarization above the dielectric transition around 440 K because it requires atomic off-centring. We have characterized the different length scales existent in  $\text{YCrO}_3$  and found that, although the average crystallographic structure above and below the dielectric transition  $\text{YCrO}_3$  is orthorhombic and centrosymmetric ( $Pnma$ ), in the ferroelectric-like state it is locally non-centrosymmetric and Cr is displaced about 0.01 Å from its position along the  $z$  direction. We conclude that the local character of the Cr off-centring and the small value of the displacement observed could explain the weak ferroelectric-like polarization. This new concept of 'local non-centrosymmetry' might be of great importance for the understanding of unusual properties of other multifunctional materials as well.

**1. Introduction**

Multifunctional materials are attracting great attention in the last few years. In particular, biferroics which are both ferromagnetic and ferroelectric are of special interest because of their potential applications [1]. The fact that ferromagnetism and ferroelectricity seem to be mutually exclusive in perovskite structure oxides and the scarcity of ferromagnetic and ferroelectric materials has stimulated a lot of theoretical and experimental work [2–4].  $\text{BiFeO}_3$  [5, 6] and  $\text{YMnO}_3$  [7–9] are long-standing examples of ferroelectrics that are also antiferromagnetic.  $\text{BiMnO}_3$  is a ferroelectric ( $T_C \sim 450$  K), which becomes ferromagnetic at 105 K [10]. On the other hand,  $\text{BiCrO}_3$  is ferroelectric ( $T_C = 440$  K) with an antiferromagnetic ground state ( $T_N = 114$  K) [11].  $\text{YCrO}_3$ , which exhibits weak ferromagnetism below  $T_N = 140$  K attributed to a canted antiferromagnetic order [12], has also recently been found to be weak ferroelectric

below  $T_C = 470$  K, where weak polarization and a dielectric anomaly were observed [13]. While it is not a genuine ferroelectric like BaTiO<sub>3</sub>, the dielectric transition at 440 K and the weak polarization somewhat resembling relaxor-like behaviour, along with canted antiferromagnetism, makes it an unusual biferroic. Moreover, theoretical studies show that the magnetic and dielectric properties are related [13]. The unusual aspect of YCrO<sub>3</sub> compared with other ferroelectrics like BaTiO<sub>3</sub> or the series PbZr<sub>1-x</sub>Ti<sub>x</sub>O<sub>3</sub>, to name a few, is that, with a crystal structure of the ABO<sub>3</sub> type, it has always been described with centrosymmetric crystal symmetries:  $P2_1/n$  [14],  $P2_1/m$  [15] or  $Pnma$  [16]. The question therefore arises as to how to reconcile the existence of ferroelectricity in this material with the centrosymmetric crystal structure, since the presence of ferroelectricity requires the displacement of the B cation relative to the oxygen cage to create an electric dipole moment. Recent first-principles density functional calculations have shown that the polarization found in YCrO<sub>3</sub> arising from the weak ferromagnetic instability is small and cannot explain the ferroelectric behaviour, and therefore local non-centrosymmetry has been suggested as the origin of the ferroelectricity in YCrO<sub>3</sub> [13]. It has been shown extensively that the pair distribution function method is an excellent method for studying local phenomena and ferroelectricity [17, 18]. In this letter, we report the results of a careful study of the local and long-range crystal structure of YCrO<sub>3</sub> using the neutron pair distribution function (PDF) and Rietveld analysis of high-resolution neutron powder diffraction (NPD) data.

## 2. Experiment

High-resolution neutron powder diffraction measurements were performed on the NPDF instrument [19] at the Los Alamos Neutron Scattering Center (LANSCE). About 3 g of YCrO<sub>3</sub> powder sample prepared as in [20] was sealed in a cylindrical vanadium can. Powder diffraction data were collected for 4 h at 550, 490, 450, 400, 295 and 15 K. Rietveld refinements were carried out using GSAS Rietveld code [21]. For PDF analysis, the data were corrected for background, incident neutron spectrum, absorption and multiple scattering, and normalized using the vanadium spectrum to obtain the total scattering structure factor  $S(Q)$ , using the program PDFgetN [22]. The PDF  $G(r)$  was obtained from  $S(Q)$  via the Fourier transform:

$$G(r) = 4\pi r[\rho(r) - \rho_0] = \frac{2}{\pi} \int_0^{Q_{\max}} Q[S(Q) - 1] \sin Qr \, dQ, \quad (1)$$

where  $\rho(r)$  and  $\rho_0$  are the atomic pair number density and average number density, respectively. The data were terminated at a value  $Q_{\max} = 35 \text{ \AA}^{-1}$ . PDF modelling was carried out using the program PDFFIT [23].

## 3. Results and discussion

Rietveld analysis of the high-resolution NPD data of YCrO<sub>3</sub> was carried out below and above the dielectric anomaly at 440 K corresponding to the low-temperature ferroelectric and high-temperature paraelectric states (figure 1). Careful Rietveld refinements confirm that the sample had no impurity and the average crystal structure is orthorhombic and not monoclinic, as reported previously [14, 15]. After detailed systematic study, we found the crystallographic space group to be  $Pnma$ , as reported in [16], and therefore centrosymmetric ( $R_{wp}$  2.4% at 300 K and 2.6% at 550 K, respectively, with  $\chi^2$  values of  $\sim 3$ ). Previously reported structural work on YCrO<sub>3</sub> was performed using x-rays [14–16] and subtle structural information important to determine the crystallographic symmetry was difficult to derive due to uncertainties in the positions of lighter atoms, resolution limitations and overall sample quality.

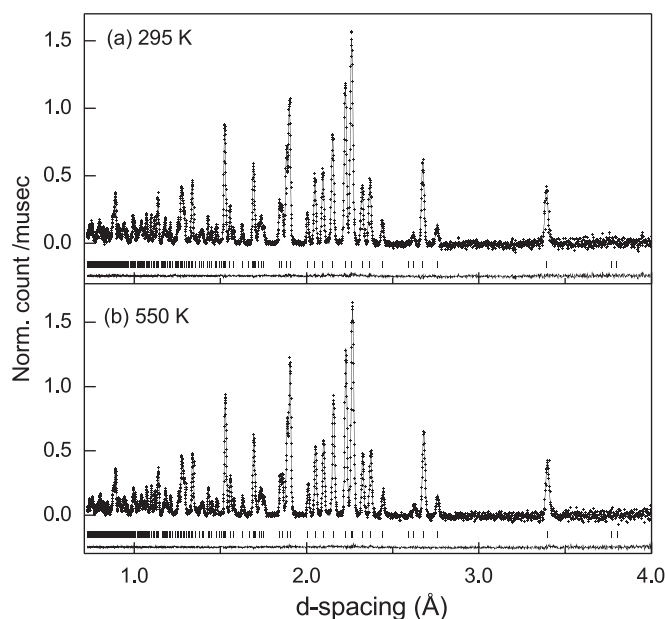


**Figure 1.** YCrO<sub>3</sub> NPD patterns obtained on NPDF in the low-temperature ferroelectric-like and high-temperature (paraelectric) states: (a) 295 K (b) 550 K. Tick marks indicate positions of the Bragg reflections. The bottom line below the tick marks is the difference between the observed and calculated NPD pattern.

It is worth mentioning that, even using the high-resolution NPD data, a slight distortion from real orthorhombic centrosymmetry is still possible within the measured uncertainties of highest symmetry. Lattice parameters and atomic positions obtained from Rietveld refinements of selected temperatures are listed in table 1.

Small variations from the ideal structure, like subtle ‘static’ or ‘quasistatic’ displacements in the atomic positions, are strongly correlated with the thermal parameters. Since Cr is in a special crystallographic position, one would expect that, if it was displaced below the ferroelectric transition (and therefore in a slightly less symmetric position), some evidence of it could be suspected from larger-than-expected values of the thermal parameters, as in the case of BaTiO<sub>3</sub> [24]. However, inspection of  $U_{\text{iso}}$  values of Cr and O shown in table 1 reveals no anomalously large  $U_{\text{iso}}$  below the ferroelectric transition.

Rietveld analysis determines the average long-range structure, since it only takes into account the intensity and position of the Bragg peaks; it cannot rule out the possibility of a different short-range or local structure, as shown by many examples [18, 25, 26]. The PDF method takes into account the information contained in the diffuse scattering of the NPD patterns. The early study of diffuse scattering revealed the existence of disordered displacements of Ti in BaTiO<sub>3</sub> [27]. Moreover, the PDF method allows the study of the different crystallographic length scales by limiting the range of a structural refinement to a certain range of distance  $r$ . For each range, structural parameters such as lattice parameters, anisotropic atomic displacement parameters, position and site occupancies are refined, therefore characterizing the different structural length scales of the system [18].

We first used the PDF method, restricting the  $r$  values to  $r_{\text{max}} = 20 \text{ \AA}$  using the  $Pnma$  space group (hereafter referred as the  $Pnma$  model). The refinement of the  $G(r)$  shows very good agreement between data and the model, as in the case of the Rietveld analysis

**Table 1.** Rietveld structural parameters for  $\text{YCrO}_3$ .  $Pnma$ : Y ( $x$ , 0.25,  $z$ ) Cr (0, 0, 0.5) O1 ( $x$ , 0.25,  $z$ ) O2 ( $x$ ,  $y$ ,  $z$ ).

	Temperature (K)		
	15	295	550
$a$ (Å)	5.5150(2)	5.5157(1)	5.5210(3)
$b$ (Å)	7.5218(3)	7.5301(1)	7.5464(1)
$c$ (Å)	5.2346(2)	5.2409(1)	5.2531(1)
$\chi^2$	3.6	2.8	3.5
$R_{wp}$ %	2.6	2.4	2.6
Y $x$	0.0668(1)	0.0662(1)	0.0654(1)
Y $z$	-0.0171(1)	-0.0171(1)	-0.0167(1)
Y $U_{\text{iso}} \times 100 \text{ \AA}^2$	0.31(1)	0.50(1)	0.78(1)
Cr $U_{\text{iso}} \times 100 \text{ \AA}^2$	0.26(1)	0.35(1)	0.53(1)
O1 $x$	0.4650(1)	0.4645(1)	0.4646(1)
O1 $z$	0.1050(2)	0.1049(1)	0.1045(1)
O1 $U_{\text{iso}} \times 100 \text{ \AA}^2$	0.35(1)	0.53(1)	0.77(1)
O2 $x$	0.3017(1)	0.3020(1)	0.3019(1)
O2 $y$	0.0538(1)	0.0537(1)	0.05334(1)
O2 $z$	-0.3063(1)	-0.3062(1)	-0.3058(1)
O2 $U_{\text{iso}} \times 100 \text{ \AA}^2$	0.38(1)	0.55(1)	0.81(1)

( $R_{wp} = 9.8\%$  at  $T = 550$  K and  $R_{wp} = 10.7\%$  at  $T = 295$  K) (figure 2). The values of  $R_{wp}$  obtained from PDF refinements are generally larger than those obtained in Rietveld refinements [18].

We then focused on the study of the local or short-range structure by restricting the  $r$  values to the range  $r_{\text{min}} = 1.6$ – $r_{\text{max}} = 6$  Å and analysing the  $G(r)$  data. In the high-temperature (paraelectric) state ( $T = 550$  K), PDF analysis over the short range agreed with the  $Pnma$  model for the local structure with  $R_{wp} = 11.0\%$  (figure 3(a)). However, in the low-temperature (ferroelectric) state, there is a clear disagreement between the PDF data and the  $Pnma$  model, as shown in figures 3(c) and (e) ( $R_{wp} = 16.3\%$  for  $T = 295$  K and  $29.1\%$  for  $T = 15$  K). Further inspection reveals that the peak at  $r = 2$  Å, which corresponds to the Cr–O distance, is much broader in the experimental PDF pattern than in the  $Pnma$  model, indicating a possible splitting of Cr–O bond lengths. Moreover, PDF peaks tend to become sharper with decreasing temperature due to reduced thermal vibrations, but our data shows that the Cr–O peaks at  $r = 2$  Å and at  $3.9$  Å do not sharpen when cooling down to 15 K. The absence of temperature dependence of the Cr–O peaks suggests that an increase in the Cr–O bond length distribution due to a more distorted structure could be compensating the effect of reduced thermal vibrations.

In order to examine the possibility of a more distorted local structure, we systematically studied possible non-centrosymmetric local structures compatible with a centrosymmetric long-range structure. Starting with  $Pnma$  structure, we looked at all possible types of distortions based on the symmetry and crystal chemistry of the perovskite structure. Initially, we tried acentric orthorhombic space groups such as  $Amm2$ ,  $Pna2_1$  and  $P2_12_12_1$ . On using the  $Amm2$  space group only the Cr atoms were displaced, while in the  $Pna2_1$  both the Y and Cr atoms are slightly displaced in order to lift the centre of inversion. However, PDF analysis did not support any of these models, because they did not produce a good fit and did not account for all the features in the local range (1–6 Å). Next we tried introducing a monoclinic distortion to the  $Pnma$  structure. PDF refinements with the  $P2_1/m$  model did not produce a good fit for

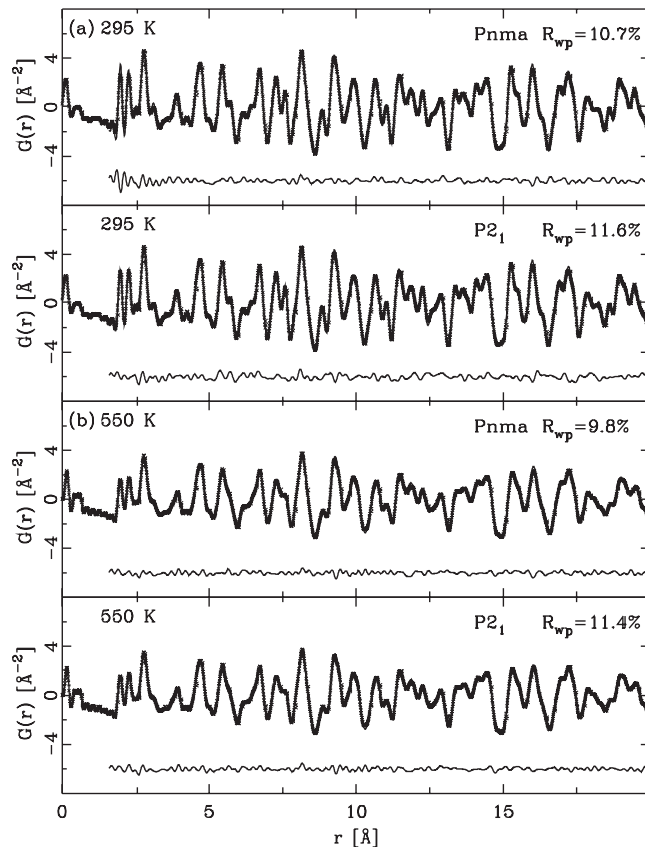


**Figure 2.** PDF refinements over the  $r_{\min} = 1.6$ – $r_{\max} = 20$  Å range for  $\text{YCrO}_3$  in the (a) low-temperature (ferroelectric) and (b) high-temperature (paraelectric) states. The space group modelled and the corresponding  $R_{wp}$  value are indicated. The difference between observed and calculated data are shown below each graph. Refinement indicates that the *Pnma* model fits better compared to *P2*<sub>1</sub> for the  $r_{\min} = 1.6$ – $r_{\max} = 20$  Å range.

the local range (1–6 Å) including the Cr–O peak (at 2 Å). We therefore lowered the symmetry from *P2*<sub>1</sub>/*m* to *P2*<sub>1</sub> by removing the centre of symmetry located at the Cr site by slightly off-setting Cr. *P2*<sub>1</sub> symmetry generates a total of ten atom sites—two Y, two Cr and six oxygen positions, with all the atoms at general positions. The key difference between the orthorhombic and the monoclinic model structures is that the Cr atoms are off-centre by 0.01 along the *c*-axis with respect to the *Pnma* space group. The Y and O positions in the *P2*<sub>1</sub> space group remain relatively close to the positions in the *Pnma* structure. The thermal parameters of all the atoms were refined. Different directions of the Cr off-centring for the two crystallographically independent Cr sites were considered, and the model that best fits the short-range data (and specially the Cr–O peak region (2 Å)) is a model with Cr off-centring along the *c*-axis.

Using the non-centrosymmetric *P2*<sub>1</sub> model to refine the short-range ( $r_{\min} = 1.6$ – $r_{\max} = 6$  Å) data in the low-temperature ferroelectric state produces a greatly improved refinement with  $R_{wp}$  values of 11.5% and 17.3% for 295 and 15 K, respectively (figures 3(d) and (f)). Moreover, the refinement was also able to capture the features in the Cr–O peak region (2 Å), indicating that the local structure is non-centrosymmetric. To make sure that the difference in  $R_{wp}$  between the *Pnma* and *P2*<sub>1</sub> models can not be attributed to the larger number of

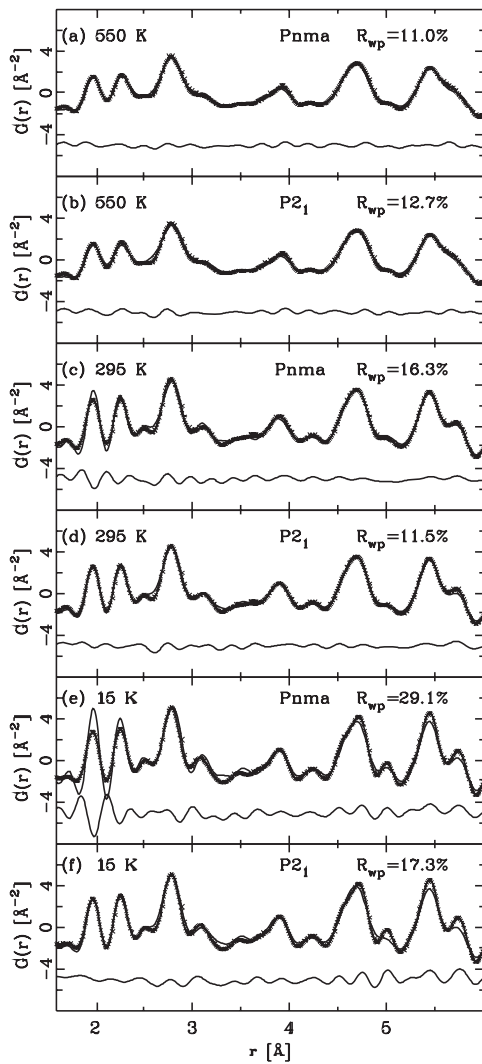


**Figure 3.** PDF refinements over the  $r_{\min} = 1.6$ – $r_{\max} = 6$  Å range for  $\text{YCrO}_3$  in the paraelectric region (550 K) ((a) and (b)) and ferroelectric region (295 and 15 K) ((c)–(f)). PDF refinements indicate that, in the paraelectric regime, the  $Pnma$  model is in better agreement with experimental data compared to  $P2_1$  while, in the ferroelectric regime, the  $P2_1$  model shows better agreement (295 and 15 K). The space group modelled and the corresponding  $R_{wp}$  value are indicated. The difference between observed and calculated data are shown below each graph.

parameters in the  $P2_1$  model, a similar refinement of the PDF data in the paraelectric state was carried out (figures 3(a) and (b)). Our analysis shows a larger  $R_{wp}$  value for the non-centrosymmetric  $P2_1$  model with respect to the centrosymmetric  $Pnma$  model ( $T = 550$  K  $R_{wp} = 12.7\%$  and  $11.0\%$ , respectively), indicating thereby that the paraelectric phase is locally centrosymmetric and that the differences between the two models obtained below the ferroelectric transition are not due to analytical artifacts. Moreover, a similar type of off-centring has been observed in many ferroelectric materials, but in all these cases the long-range and the short-range structures were non-centrosymmetric [28, 29]. This off-centring model was also found to be the lowest energy structure for  $\text{YCrO}_3$  by first-principles spin-dependent density functional theory calculations [13].

In order to characterize the Cr off-centring, a series of systematic refinements with different values of the Cr displacement along the  $z$  direction was performed at different temperatures and the  $R_{wp}$  values were recorded (figure 4). A clear minimum in the  $R_{wp}$  values was obtained for a Cr displacement of about  $0.01$  Å along the  $z$  direction at 15 and 295 K, indicating the existence

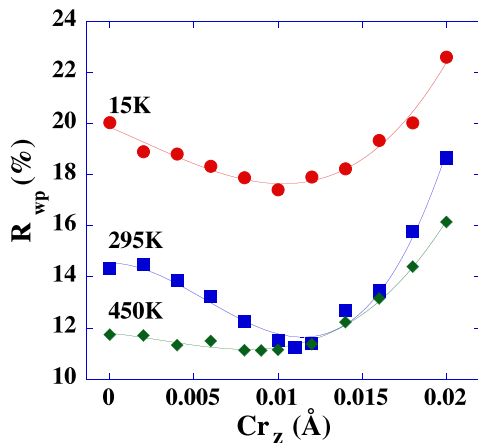


**Figure 4.**  $R_{wp}$  values obtained from PDF method ( $r_{\max} = 6 \text{ \AA}$ ) as a function of Cr displacement along the  $z$  direction in the low-temperature ferroelectric-like state of  $\text{YCrO}_3$ . (This figure is in colour only in the electronic version)

of a small static or quasistatic local Cr off-centring. It is worth noticing that the value of the displacement is ten times smaller than the local distortions observed in  $\text{PbZrO}_3$  [30, 31]. This analysis allowed us to relate the local non-centrosymmetry to the ferroelectric transition temperature, since the same study performed with the data obtained 20 K below the ferroelectric temperature (450 K) shows the same kind of behaviour but with a shallower minimum at about the same displacement value. If such an order-of-magnitude displacement (0.01 Å along the  $z$  direction) occurred coherently throughout the material, Rietveld analysis of the high-resolution neutron diffraction data would have converged better using the non-centrosymmetric model. This evidence makes us conclude that the off-centring of Cr atoms happens in a disordered manner and is therefore local.

The above results indicate that, in the low-temperature ferroelectric state,  $\text{YCrO}_3$  is locally non-centrosymmetric. Our results demonstrate the existence of local non-centrosymmetry in the low-temperature phase of  $\text{YCrO}_3$ , although the average crystal structure is centrosymmetric. It is not yet clear what is the origin of the off-centring displacement of the Cr atom in  $\text{YCrO}_3$ . However, the small value of the Cr off-centring displacement and the local character of the non-centrosymmetry nature in  $\text{YCrO}_3$  could explain the small value of the polarization observed in this material ( $2 \mu\text{C cm}^{-2}$  at 300 K for  $\text{YCrO}_3$  compared to  $25 \mu\text{C cm}^{-2}$  in  $\text{BaTiO}_3$ ). It is likely that the same type of local non-centrosymmetry may give rise to ferroelectricity and related phenomena in other materials as well. A case in point is  $\text{BiMnO}_3$ , which is shown experimentally to be a biferroic, although the non-centrosymmetric  $C2$  space group is not clearly established [32–34]. It could be globally centrosymmetric with the  $C2/c$  space group and locally non-centrosymmetric with the  $C2$  space group. This would also account for the low value of the polarization in  $\text{BiMnO}_3$ .

#### 4. Conclusions

In summary, our high-resolution neutron powder diffraction data reveal an average centrosymmetric structure for  $\text{YCrO}_3$  with space group  $Pnma$  both above and below the dielectric transition temperature. However, using neutron pair distribution function analysis we found that, in the low-temperature ferroelectric-like state,  $\text{YCrO}_3$  is locally non-centrosymmetric, characterized with a Cr off-centring displacement of the order of 0.01 Å along the  $z$  direction that seems to be temperature independent. We have shown that local non-centrosymmetry may indeed be very important in understanding the properties of multifunctional materials, and that this needs to be explored further.



This work has benefited from the use of NPDF at the Lujan Center at the Los Alamos Neutron Science Center, funded by the Office of Basic Energy Sciences of the US Department of Energy (DOE). The Los Alamos National Laboratory is operated by Los Alamos National Security LLC under DOE contract DE-AC52-06NA25396. The upgrade of NPDF has been funded by the US National Science Foundation through grant DMR 00-76488. The authors thank A K Kundu for preparing the YCrO<sub>3</sub> sample.

## References

- [1] Wood V E and Austin A E 1975 *Magnetoelectric Interaction Phenomena in Crystals* ed A J Freeman and H Schmid (London: Gordon and Breach)
- [2] Spaldin N A and Fiebig M 2005 *Science* **309** 391
- [3] Hill N A 2000 *J. Phys. Chem. B* **104** 6694
- [4] Kimura T, Goto T, Shintani H, Ishizaka K, Arima T and Tokura Y 2003 *Nature* **426** 55
- [5] Sosnowska I, Peterlin-Neumaier T and Steichele E 1982 *J. Phys. C: Solid State Phys.* **15** 4835
- [6] Wang J *et al* 2003 *Science* **299** 1719
- [7] Huang Z J, Cao Y, Sun Y Y, Xue Y Y and Chu C W 1997 *Phys. Rev. B* **56** 2623
- [8] Fiebig M, Lottermoser Th, Lonkai Th, Goltsev A V and Pisarev R V 2005 *J. Magn. Magn. Mater.* **290** 883
- [9] Aken B V, Palstra T M, Filippetti A and Spaldin N A 2004 *Nat. Mater.* **3** 164
- [10] Moriera dos Santos A, Cheetham A K, Atou T, Syono Y, Yamaguchi Y, Ohoyama K, Chiba H and Rao C N R 2002 *Phys. Rev. B* **66** 064425
- [11] Nitata S, Azuma M, Takano M, Nishibori E, Takata M and Sakata M 2004 *Solid State Ion.* **172** 557
- [12] Judin V M and Sherman A B 1966 *Solid State Commun.* **4** 661  
Morishita T and Tsushima K 1981 *Phys. Rev. B* **24** 341
- [13] Serrao C R, Kundu A K, Krupanidhi S B, Waghmare U V and Rao C N R 2005 *Phys. Rev. B* **72** 220101(R)
- [14] Katz L 1955 *Acta Crystallogr.* **8** 121
- [15] Looby J T and Katz L 1954 *J. Am. Chem. Soc.* **76** 6029
- [16] Geller S and Wood E A 1956 *Acta Crystallogr.* **9** 563
- [17] Kwei G H and Billinge S 1995 *Ferroelectrics* **164** 57–73
- [18] Egami T and Billinge S J L 2003 *Underneath the Bragg-Peaks: Structural Analysis of Complex Materials* (Amsterdam: Elsevier Science)
- [19] Proffen Th, Egami T, Billinge S J L, Cheetham A K, Louca D and Parise J B 2002 *Appl. Phys. A* **74** S163
- [20] Rao G V S, Wanklyn B M and Rao C N R 1971 *J. Phys. Chem. Solids* **32** 345
- [21] Larson A C and Von Dreele R B 2000 *Los Alamos National Laboratory Report No.* LAUR 86-748  
Toby B H 2001 *J. Appl. Crystallogr.* **34** 210
- [22] Peterson P F, Gutmann M, Proffen Th and Billinge S J L 2000 *J. Appl. Crystallogr.* **33** 1192
- [23] Proffen Th and Billinge S J L 1999 *J. Appl. Crystallogr.* **32** 572
- [24] Kwei G H *et al* 1993 *J. Phys. Chem.* **97** 2368–77
- [25] Rodriguez E E, Proffen Th, Llobet A, Rhyne J J and Mitchell J F 2005 *Phys. Rev. B* **71** 104430
- [26] Proffen Th, Billinge S J L, Egami T and Louca D 2003 *Z. Kristallogr.* **218** 132
- [27] Comes R *et al* 1968 *Solid State Commun.* **6** 715  
Comes R *et al* 1970 *Acta Crystallogr. A* **26** 244
- [28] Egami T, Momontov E, Dmowski W and Vakhrushev S B 2003 *Fundamental Physics of Ferroelectrics; AIP Conf. Proc.* **677** 48
- [29] Jeong I-K, Darling T W, Lee J K, Proffen Th, Heffner R H, Park J S, Hong K S, Dmowski W and Egami T 2005 *Phys. Rev. Lett.* **94** 147602
- [30] Dmowski W, Egami T and Farber L 2002 *Fundamental Physics of Ferroelectrics; AIP Conf. Proc.* **582** 33
- [31] Teslic S and Egami T 2003 *Acta Crystallogr. B* **54** 750
- [32] Belik A A *et al* 2006 *J. Am. Chem. Soc.* **128** 706
- [33] Baettig P and Spaldin N A 2007 private communication
- [34] Atou T, Chiba H, Ohoyama K, Yamaguchi Y and Syono Y 1999 *J. Solid. State Chem.* **145** 639